WAVES AND THEIR EFFECT ON CONVECTIVE GAS DIFFUSION IN DISCHARGING FLUID FILMS

V. E. Nakoryakov, B. G. Pokusaev, and K. B. Radev

UDC 66.071.:532.59

It is well known that waves formed by instabilities at the surface of freely discharging fluid films intensify substantially the processes of interphase heat and mass transfer. It has been shown in direct experiments [1, 2] that during desorption from laminar-wave fluid films of weakly dissolved CO_2 gas the mass-transfer coefficient due to waves is enhanced by more than twice, and this effect depends on both the period and the amplitude of the stationary two-dimensional waves.

It is noted that since for weakly dissolved gases the main resistance is concentrated in the fluid phase, the diffusion process in the gas can be neglected. However, the information obtained in these studies was insufficient for proper verification of the full theoretical models [3-5], constructed for large values of the Schmidt number $Sc = \nu/D$ (D is the diffusion coefficient) within the approximation of a thin diffusion boundary layer near the free surface.

The mass-transfer experiments in [2] were carried out only for low values of the numbers $Re \leq 40$ ($Re = q_0/\nu$, where q_0 is the specific fluid discharge, and ν is the kinematic viscosity) with fixed wave parameters in the two-dimensional wave regime. In real situations these two-dimensional waves exist only at the initial portion of wave generation and growth, and a chaotic three-dimensional nonlinear wave regime [5] develops further with length, as the two-dimensional waves are deformed very strongly.

The study of dynamics of such waves is of independent interest in developing the theory of nonlinear dispersion waves. On the other hand, it is obvious that in studying interphase mass transfer it is necessary to know well the structure and all wave characteristics in the experimentally realized wave regime. Precisely these studies were carried out in the present study for vertically discharging fluid films with $Re \leq 400$. New information is obtained concerning the effect of wave dynamics on transport processes as a whole, and, in particular, the variation of the intensification factor of this process as a function of length of the film surface with variation of the wave characteristics and of Re.

The experimental results are compared with the asymptotic theoretical models, and the mass-transfer intensification mechanism by waves is discussed in detail.

1. Experimental Technique. The experiments were performed on the instrumentation of [2, 5]. The fluid film discharges from a coaxial annular gap of width 0.5 mm long a vertical steel cylinder of diameter 60 mm and length 1 m. The fluid is saturated vertically by a CO_2 gas, is thermally stabilized at a level of 20°C, and reaches the operating portion through the discharge-measuring instrument from a constant-level reservoir. The wave parameters and the local gas concentration are also measured as a function of length during the experimental process.

Measurements of the local film width were carried out by a shadow method, in which, unlike the method described in [5], the light source was taken to be plane-parallel laser radiation, with the use of photoelectron recording of the optical signal. This photoelectric method makes it possible to measure the film width with an error varying from 0.5 to 5%, the wave amplitude within 1%, and the period and phase velocity within 1% too.

The measurement of the mean mass-transfer coefficient was carried out by a conductometric method [6]. The essence of this method is that the ratio of electric signals of two special platinum electrochemical detectors, placed in the fluid in the distributing input instrument and in the mobile liquid sample, is a step function of the CO_2 concentration ratio at the inlet C_0 and outlet C_L of the mass-transfer portion of length L.

Novosibirsk. Translated from Zhurnal Prikladnoi Mekhaniki i Tekhnicheskoi Fiziki, No. 3, pp. 95-104, May-June, 1987. Original article submitted March 14, 1986.

0021-8944/87/2803-0404$12.50

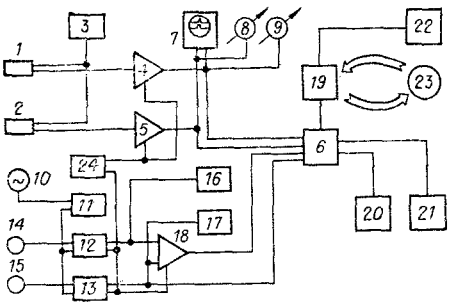

Fig. 1

Thus, the mass-transfer coefficient upon desorption $k_L = (q/L)\ln(C_0/C_L)$, obtained from the balance of the gas dissolved in the film, is proportional to the logarithm of ratio of signals U_0^*, U_L^* at the inlets of the corresponding amplifiers: $k_L = P(q/L)\ln(U_0^*/U_L^*)$, where P is a temperature-dependent coefficient (0.5-1) determined as a result of calibration measurements. The total error in determining the Sherwood number $Sh = k_L h_0/D$ was 0.6-2.7%. This method was verified experimentally.

The selection and handling of signals of the two amplifiers of the constant-current shadow device and of the two conductometric amplifiers, along with the data analysis of the current values of the length, temperature, solvent discharge, and physical properties of the fluid and gas, were carried out in an automatic measurement complex.

The measurement complex, whose block diagram is shown in Fig. 1, consists of a shadow device: photomultipliers 1 and 2, high-voltage power supplies 3 and 24, constant-current amplifiers 4 and 5, a two-beam oscillograph 7 and voltmeters 8 and 9; a conductometric device: a low-frequency generator 10, a precision separator 11, electrochemical detectors 14 and 15, measurement amplifiers 12 and 13, integrating voltmeters 16 and 17, and a difference amplifier 18; and a universal computing complex (UCC M 6000) 19, to which are attached a KAMAK crate 6 with a terminal 20 and a graph display 21, a printer 22, and a magnetic disk unit 23. All three sections can operate autonomously.

In establishing the graph of the film thickness as a function of time, we used the phase method of the structural averaged signal, making it possible to extract the characteristic structures of the separation structure under conditions of a stochastic wave process and thus to obtain their generalized "portraits." The printer's interrogation period was determined in this case primarily from data on the maximum signal frequency, measured by a spectrum analyzer. The averaging was carried out over the characteristic phase of the signal $H = h_0(t, x_0, z_0) - \langle h \rangle$, more precisely, $\{H > 0, H = 0\}$.

The methodology of measuring the mass-transfer coefficient was carried out by measuring the gas inlet from the smooth film $1 - C_0/C_L$ and comparing it with calculation results of permeation theory and with exact calculations of convective diffusion equations [7]. The difference between measurements and calculations did not exceed 3-5%.

The physical properties of the fluid and the gas (surface tension σ, density ρ, viscosity ν) were determined from known tabulated data and controlled directly during the experiments by means of standard methods. To calculate the diffusion coefficient we used the dependence of [8], generalizing all known experimental and theoretical results for $D = 132 \cdot 10^{-15}/v_g f_i \mu^{B_i}$, where v_g is the molar volume of the gas, and f_i and B_i are constants depending on the type of the fluid. Thus, for CO_2, $v_g = 37.3$ m^3/mole, and for water $f_i = 1.0$, $B_i = -1.15$.

In order to avoid dependences of the diffusion coefficient on the concentration of the dissolving gas, the experiments on desorption of carbon dioxide gas were carried out at concentrations of 50-500 mg/liter, which is substantially less than the saturated fluid concentration.

2. Inherent Chaotic Waves. As is well known [5], in the Re region from 3-7 to 400 one observes a stable laminar-wave flow regime, characterized by the generation of perturbations following the smooth portion, leading to formation of linear and nonlinear two-dimensional waves. Further, at distances of the order of several wavelengths they decompose into three-dimensional chaotic waves propagating downward along the formation flow.

Using the phase-averaging method on the signal of the fluid-film thickness, generalized "portraits" were obtained of these coherent perturbation structures of the film surface. Figure 2 shows in the coordinates (h, t)

TABLE 1

Re	⟨h⟩, msec	T, msec	λ, mm	c, m/sec	Re	⟨h⟩, μm	T, msec	λ, mm	c, m/sec
14,5	150	47,1	43,1	0,914	87,9	346	20,9	446	21,3
18,0	153	32,5	240	7,49	112	356	18,7	30,2	1,61
22,3	152	37,8	33,9	0,898	144	389	21,3	28,6	1,34
27,5	171	28,8	40,8	1,42	178	412	18,7	36,0	1,92
35,2	171	26,3	25,6	0,974	226	438	16,1	36,1	2,24
43,9	190	27,8	137	4,94	288	474	11,8	23,5	1,99
56,6	238	29,6	15,6	0,524	352	460	12,2	33,5	2,75
68,2	269	30,4	154	5,05	440	470	8,79	82,5	9,39

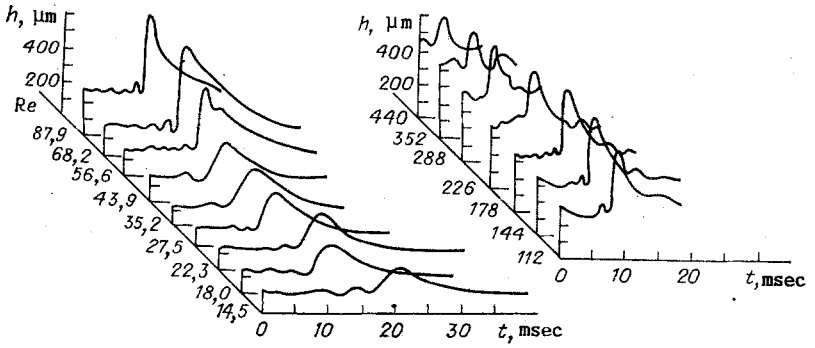

Fig. 2

characteristic wave profiles, removed from the lines of wave formation by a distance of 260 mm from the fluid inlet (water, $Fi^{1/11} = 8.79 \pm 0.02$, $Fi = \sigma^3/\rho^3 g\nu^4$) , as a function of Re, while Table 1 provides generalized data, respectively, for the mean film thickness ⟨h⟩ , the period T, the longitudinal component of the phase velocity c, and the "wavelength" $2\pi h_0/k$ (k is the wave number, and h_0 is the Nusselt thickness) of these structures for Re.

Until the transition to the turbulent flow regime the waves have the shape of independent identical surface perturbations with a steep front and mild retarded fronts. With increasing Re the wave amplitude $A = h_*/h_0$ increases, achieves maximum values for Re ≃ 20-70, and again decreases. In this case a lump is formed at the retarded front of the structures, which for large Re decays into a residual layer and decomposes into two waves of small amplitude. The amplitude of these formations increases, while that of the fundamental wave decreases. In the transition region to the turbulent regime (for Re → 350-400) the amplitudes become commensurate, and the shapes are more symmetric. A similar evolution of the structural shape is found according to the classification of film regime flows (carried out, for example, in [9]) by the variation of the maximum and mean film widths with Re. The Re dependences of the mean film thickness and of the amplitude, dimensionless in the Nusselt thickness $h_0 = (3\nu^2/g)^{1/3}Re^{1/3}$ of a smooth film, and of the wave periods and their phase velocities are also found in good agreement with the data of [10-12]. As is seen from Fig. 2 and Table 1, an extremum in the behavior of wave characteristics is observed in the region of values Re = 50-100, related, obviously, to the rearrangement of the structural profiles, a coarsening of their leading front, and an increase in the relative wave amplitude. All this leads to a substantial contribution of nonlinearity to the general pattern of wave evolution.

The appearance of nonlinear dispersion effects in the regime of three-dimensional wave flow can be illustrated in Fig. 3, where we illustrate measurements of c/u_0 values as a function of $kA = 2\pi h_*/\lambda$. As is indicated, the data are generalized by the dependence $c/u_0 \sim (kA)^p$, similar to that obtained in [5, 13]. Here $p = -1$ for the structures (line 1) and $p = -0.46$ for two-dimensional waves (using in 2 Re = 10-31, $Fi^{1/11} = 9.2$, and in 3 the data of [13] for Re = 4—12, $Fi^{1/11} = 3.55$, $Fi = \sigma^3/(\rho^3 g\nu^4)$).

Simultaneously with studying wave dynamics of an inherently discharging film, dependences were obtained of the intensification factor of mass transfer Sh/Sh_0 as a function of Re at Sc = 582 for sixteen values of the length L of the mass exchange portion, several of which are shown in Fig. 4. Here we used the expression as the mass-transfer coefficient for a smooth film $Sh_0 = \sqrt{6h_0 Pe/\pi L}$, where the Peclet number is Pe = q/D.

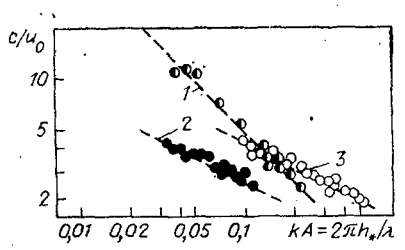

Fig. 3

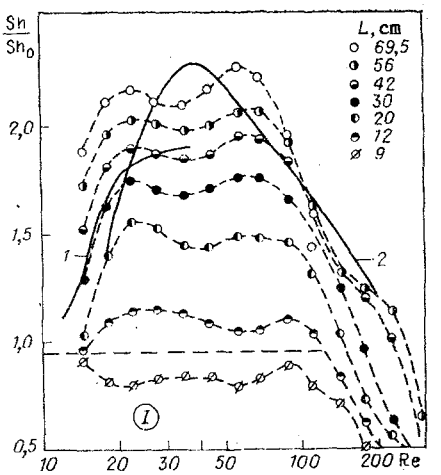

Fig. 4

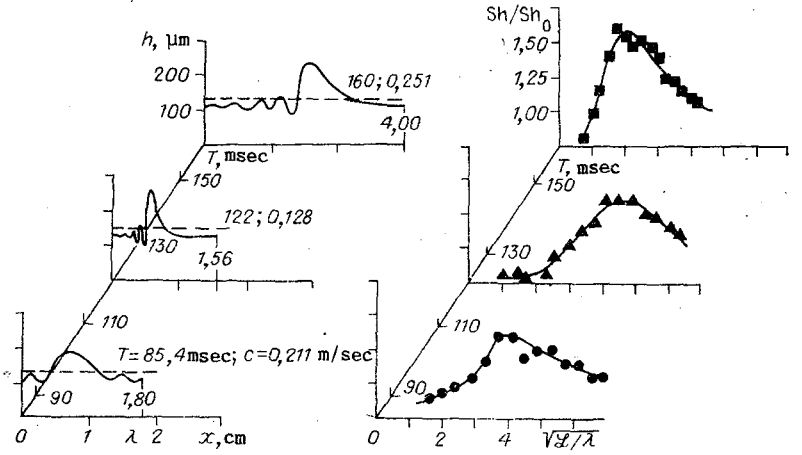

Fig. 5

We proceed to analyze these results. As is seen, except for the initial portion (region I in Fig. 4), for all investigated lengths of the mass-transfer portion, the relative mass-transfer coefficient initially increases substantially with increasing Re until Re $\sim$ 20-30, while for Re $>$ 100 it is substantially reduced to $Sh/Sh_0 \lesssim 1$. A comparison has been provided between experimental data and the results of [2] (line 1, Sc = 3750, L = 29.5 cm) and [14] (line 2, Sc = 600, L = 57 cm). Good agreement is noticed in the general tendencies of the dependences for each of the comparable experimental conditions, and the result of [2] concerning the growth in the intensification factor with increasing Sc has been verified (for otherwise equal conditions). The effect of the portion of flow establishment at the input is expressed in the low values of the intensification factor ($Sh/Sh_0 < 1$) up to values L = 9-12 cm for Re $\leq$ 100. On the other hand, it is known that the occurrence of waves at the film surface at these Re values takes place at distances of 5-10 cm from the input [5]. It is clear that at these distances the increase in the mass-transfer coefficient from zero at L = 0 occurs due to both the establishment of a semiparabolic velocity profile and to wave formation. We note that for an inclined film the evolution of a velocity profile and of waves occurs at longer distances from the inlet; therefore, the intensification factor must be smaller than on a vertical wall.

3. Quasistationary Excited Waves. For maximum length of the operating portion (L = 70 cm) the contribution of the initial portion to the mean mass-transfer coefficient is significant. To eliminate this effect, modeling was undertaken of the waveflow regimes by quasistationary excited fluctuations of the discharging fluid. The possibility of this modeling was illustrated in [5], where it was shown that the wave regime is established at distances of the order of a wavelength from the aperture of the gap from which the film flows. The advantage of this approach is that the problem of theoretical modeling of the mass-transfer process is facilitated. In this case it must be remembered that the excited waves retain the two-dimensionality and periodicity for Re not exceeding 30-40.

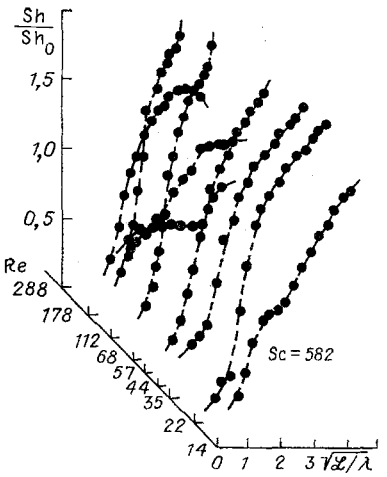

Fig. 6

The properties of two-dimensional quasistationary waves have been investigated quite well [5]. Therefore, we note here only the nonlinearity of the stationary excited waves (lines 2, 3 in Fig. 3) and the small contribution (~4%) of waves to the relative surface enhancement (length $\mathcal{L}$) of the phase separation boundary.

Figure 5 shows the experimental results of investigating waves and mass transfer at Re = 10 for three waveflow regimes. On the left are shown the excited wave profiles and their wave characteristics, and on the right the corresponding dependences of the intensification factor $\sqrt{\mathcal{L}/\lambda}$ (for a smooth film $Sh_0 \sim 1/\sqrt{\mathcal{L}}$). In the plots one can trace the characteristic linear increase of Sh/Sh_0 with $\sqrt{\mathcal{L}/\lambda}$ at short distances from the inlet. Further, reaching saturation, the functional dependence starts decreasing, and can acquire again values of the order of 1. Similar experimental dependences of Sh/Sh_0 on dimensionless length (selected from Fig. 3 for chaotic waves), obtained in the regimes corresponding to those shown in Fig. 2, are shown in Fig. 6.

As seen by comparing the plots, the shape of the dependence of Sh/Sh_0 on $\sqrt{L/\lambda}$ is determined by the wave characteristics of the flow. Tracing the variation of this function with wave velocity and amplitude, it can be noted that torsion in the initial portion of the curves and large absolute values of the maximum intensification factor are achieved for large values of wave velocity and amplitude and for longer waves with smaller wave number. This fact was first noted in [1, 2]. As to flows with chaotic waves, as seen from Fig. 6, as a whole the nature of increase in the mass-transfer intensification factor (Sh/Sh_0) with length is retained, though, as shown below, the role of the initial hydrodynamic and mass-transfer portions is more substantial in this case than for quasistationary two-dimensional waveflow.

4. Model of the Transport Process. Similarly to the problem investigated for a smooth film, in the diffusion problem of a weakly dissolved gas we consider two limiting cases of values of the phase contact time $\theta = L/h\,Pe$: $\theta \ll 1$ and $\theta \sim 1$. At $\theta > 1.67$ the film is already fully saturated by the gas (for absorption) or by depletion (for desorption).

The analysis of gas diffusion in a discharging wave film with $\theta \ll 1$ was carried out in [3, 4]. Analysis of the problem with $Pe \gg 1$ shows that for long waves ($\varepsilon = \langle h \rangle/\lambda \ll 1$) of large amplitude with $Sc \sim 1/\varepsilon^2$, $Re \sim 1 - 1/\varepsilon^2$, in the transport equation written in the coordinates ($\xi = x - ct$, $\chi = \int_0^x \sqrt{1+h_x^2}\,dx$, $\eta = \sqrt{1+h_x^2}(h-y)$,

it is necessary to take into account the curvature of the phase separation surface, which is expressed in terms of corrections of order ε and ε^2 to the coefficients in front of the derivatives.

For stationary waves the problem is written in the form

$$\frac{\partial C}{\partial \xi} + \frac{U_S}{W_S}\frac{\partial C}{\partial \chi} = \frac{W_S}{\varepsilon\,Pe}\frac{\partial^2 C}{\partial \psi^2},$$
$$\chi = 0,\ C = 1;\ \psi = 0,\ C = 0;\ \psi \to \infty,\ C \to 1, \tag{4.1}$$

where $C = (C - C_S)/(C_0 - C_S)$; $W_S = U_S$ is the surface velocity in a coordinate system attached to the wave, $\psi = -\int_0^{\eta} U d\eta$; we used the condition of absence of tangential stresses at the surface $\partial u/\partial\psi = 0$ for $\psi = 0$, and S is the value of the quantity at the separation surface. Solving the system (4.1) by the methods used in the references quoted, we obtain after averaging the gas flow over the phase ξ and the length $\mathscr{L}$ of the surface

$$\frac{\mathrm{Sh}}{\mathrm{Sh}_0} = -\sqrt{\frac{2}{3\mathscr{L}}}\int_0^1 \frac{au_S}{W_S}\left\{\int_{g_1(\mathscr{L}+f_1(\xi))}^{\xi} W_S d\xi\right\}^{1/2} d\xi. \tag{4.2}$$

Here $\mathscr{L} = L\int_0^1 \sqrt{1+\varepsilon^2 h_x^2}\,dx$; $\mathrm{Sh}_0 = \sqrt{6\varepsilon \mathrm{Pe}/\pi\,\mathscr{L}}$ is the mass-transfer coefficient of a smooth film of length $\mathscr{L}$ and width $\langle h\rangle$, and $g_1 = f_1^{-1}$; $f_1(\xi) = \int_{\xi}^{0} \frac{U_S a}{W_S} d\xi$. According to [4], for $\mathscr{L} \ll 1$ the expansion of the lower limit of the integral in (4.2) in a series leads to $g_1(\mathscr{L} + f_1(\xi)) = \xi + \mathscr{L}/f_1'(\xi) + O(\mathscr{L}_2) = \xi - W_S\mathscr{L}/UU_S + O(\mathscr{L}_2)$. The minimum values of the intensification factor are then

$$\left(\frac{\mathrm{Sh}}{\mathrm{Sh}_0}\right)_{\mathscr{L}\to 0} = \sqrt{\frac{2}{3}}\int_0^1 U_S^2 d\xi. \tag{4.3}$$

At the points $\mathscr{L}_m = mf_1(\xi)$ $(m = 1, 2, \ldots)$ expression (4.2) acquires the value

$$\left(\frac{\mathrm{Sh}}{\mathrm{Sh}_0}\right)_* = \left(\frac{2}{3}\frac{L}{\mathscr{L}} f_1(1)\int_1^0 W_S d\xi\right)^{1/2}, \tag{4.4}$$

since $g_1(mf_1(1) + f_1(\xi) = \rho_1(f_1(m + \xi)) = m + \xi$. Expressions (4.3) and (4.4) are independent of the number of waves at the mass-transfer portion, with values both smaller and larger than unity.

The results obtained above differ from the data of [4] only in that here, by means of $W_S = \sqrt{1+\varepsilon^2 h_x^2}\, w_S + c$, $U_S = u_S + \varepsilon^2 h' v_S$ within the approximate equation we accounted for the effect of the curvature of the separation surface, which is substantial for large-amplitude waves for moderate Re.

In the case of moderate values of the phase contact time in a smooth film with $\theta > 0.1$ a variation of the gas concentration occurs over the whole film thickness. It is assumed that this condition is also satisfied during wave motion of the film surface

$$C(\xi, x, \zeta) = -j(\xi, x)\varphi(\zeta), \quad \zeta = 1 - \gamma/h(\xi),$$

where the function φ is given as

$$\varphi(\zeta) = \sum_{n=1}^{\infty} b_{2n-1}\zeta^{2n-1}, \quad b_1 = 1, \quad b_3 = \frac{3}{2}\beta_1^2\frac{-b_1}{2,3}, \quad b_{2n+1} = \frac{3}{2}\beta_1^2\frac{b_{2n-3} - b_{2n+1}}{2n(2n+1)},$$

$$\beta_1^2 = 3{,}4144$$

and satisfies the following conditions at the free boundary and at the solid wall

$$\varphi(0) = 0, \quad \varphi^1(0) = 0.$$

Using the usual assumption of local semiparabolic velocity profile of the film, integration across the fluid layer leads to the problem of determining the gas flow density through the separation boundary:

$$\frac{\partial j}{\partial\xi} + \frac{\alpha u_S}{w_S}\frac{\partial j}{\partial x} = \left(\frac{\beta}{h^2} - w_S'\right)\frac{j}{w_S}, \quad x = x_0, \; j = j_0(\xi),$$
$$\gamma = \int_0^1 \varphi d\zeta, \; \alpha = \int_0^1 f\varphi d\zeta/\gamma, \; \beta = \varphi^1(0)/\varepsilon\,\mathrm{Pe}\,\gamma, \; \varphi^1(0) = 1, \; f(\zeta) = 1 - \zeta^2. \tag{4.5}$$

The solution of (4.5) is

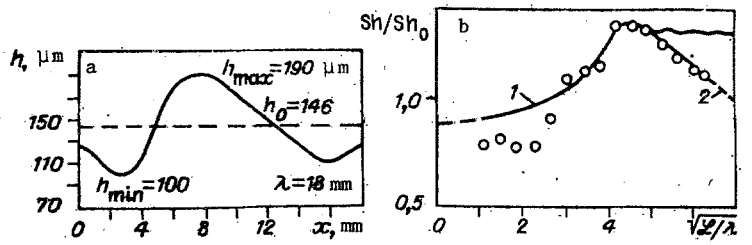

Fig. 7

$$j(\xi, x) = j_0(\xi)\frac{w_S[g_2(x - x_0 + f_2(\xi))]}{w_S(\xi)_j}\exp\left\{\beta\int\limits_{g_2(x-x_0+f_2(\xi))}^{\xi}\frac{d\xi}{w_S h^2}\right\},$$

$$g_2 = f_2^{-1},\ f_2(\xi) = \alpha\int\limits_{\xi}^{0}\frac{u_S}{w_S}d\xi,\ w_S = \alpha u_S - c.$$

For $\theta \geq 0.1$ the mass-transfer coefficient of a smooth film is given by the following expression with an error not exceeding 2%

$$\mathrm{Sh}_0 = -\ln[R_1\exp(-\beta_1^2\theta)]/\theta,\ R_1 = 0{,}8056,\ \beta_1^2 = 3{,}41$$

and the intensification factor is written in the form

$$\frac{\mathrm{Sh}}{\mathrm{Sh}_0} = (3.41 + 0.216\theta)^{-1}\left[\frac{x_0}{L}\theta\,\mathrm{Sh}_1 + \frac{\gamma}{L - x_0}\int\limits_0^1 j_0(\xi)\frac{[w_S + 1 - c]\,h^2}{1 - u_S'h^2/\beta}\times\right.$$
$$\left.\times\left\{1 - \frac{c - \alpha u_S(g_2(L - x_0 + f_2))}{c - \alpha u_S(\xi)}\exp\left[\beta\int\limits_{g_2(L-x_0+f_2)}^{\xi}\frac{d\xi}{w_S h^2}\right]\right\}d\xi\right], \tag{4.6}$$
$$\alpha = 0{,}59,\ \beta = 1/\gamma\varepsilon\mathrm{Pe},\ \gamma = 0{,}316.$$

One easily obtains expressions for the intensification factor at the points $L_m - x_0 = mf_2(1)$ (m = 1, 2, 3,...), since $g_2(L_m - x_0 + f_2(\xi)) = g_2(f_2(m + \xi)) = m + \xi$:

$$\left(\frac{\mathrm{Sh}}{\mathrm{Sh}_0}\right)_m = (3.41 + 0.216\theta)^{-1}\left[\frac{x_0}{L_m}\theta\,\mathrm{Sh}_1 + \frac{\gamma}{L_m - x_0}\int\limits_0^1\frac{(w_S + 1 - c)\,h^2}{1 - u_S'h^2/\beta}j_0(\xi)\left\{1 - \exp\left[m\beta\int\limits_1^0\frac{d\xi}{w_S h^2}\right]\right\}d\xi\right]. \tag{4.7}$$

Since $w_S < 0$, expression (4.7) decreases with increasing m; therefore, $(\mathrm{Sh}/\mathrm{Sh}_0)_{m+1} < (\mathrm{Sh}/\mathrm{Sh}_0)_m$.

5. Comparison with Experiment. Calculations by Eqs. (4.2) (line 1 in Fig. 7b) and (4.6) (line 2) for the wave (Fig. 7a) recorded in the experiment are compared in Fig. 7b with measured values of $\mathrm{Sh}/\mathrm{Sh}_0$ for Sc = 578, Fi = $3.85 \cdot 10^{10}$, Re = 10, T = 85.4 msec, $c/u_0 = 3.2$.

The film surface velocity has been established under the assumption of retaining the discharge at the distance of one wavelength [5]. The gas flow density $j_0(\xi)$ in (4.7) was determined by solving (4.1) at $L = x_0$, and for Sh_1 we selected the Sh value at $x_0 = 20.0$ (36 cm). Good qualitative agreement can be noted between the experimental and model dependences both for the initial ($\theta < 0.044$) and for the evolved ($\theta > 0.1$) diffusion portion.

It was shown theoretically in [4, 15] that the effect of waves on diffusion of a weakly dissolved gas in a discharging film is related to the increase in the local gas flow in troughs at the trailing fronts of the waves, where the fluid flows toward the free surface. This is related to compression in the troughs and expansion in the crests of the current lines, carried out during wave motion below the flow.

In interpreting the dependences obtained, an important quantity is the drift time of the wave system with respect to the flow, which can be defined as $\tau_d = \int\limits_0^\lambda d\xi/(c - u_S)$. In the laboratory coordinate system this time corresponds to a distance $L_1 = c\int\limits_0^\lambda d\xi/(u_S - c)$ from the inlet, on which the fluid under the (i + 1)-th wave is totally displaced by the fluid found at the beginning of the motion under the i-th wave, and, consequently, is depleted

by the gas (in the case of its desorption). Depending on the relationship of L_1 values, the current lengths of the mass-exchange portion L, and the diffusion-layer length $L_d \leq 0.067 h_0$ Pe (the equality corresponds to a smooth film), a different behavior of Sh and Sh/Sh_0 with varying dimensionless distance from the inlet (number of waves on the film) is observed. This is related to the effect of the velocity profile in the film on the evolution of the concentration profile near the free surface.

At distances $L \lesssim L_1 \ll L_d$ the diffusion layer is thin, and each of these distances leads to a maximum increase of the local gas flow, while in this region $Sh/Sh_0 \sim (L/\lambda)^{1/2}$ (curve 1 in Fig. 7). With further increase in L the width of the diffusion layer is enhanced and the drift time is shortened, leading in turn to reduced values of the local maxima of the intensification factor [4]. It is precisely this mechanism which underlies the continuous increase in Sh/Sh_0 predicted in [4] for $u_S \simeq c$. For $L > L_d$ the intensification factor (delaying its growth) reaches maximum values and decreases, but the slower it is, the longer is the drift time.

The transverse velocity fluctuations in the leading wave front increase with increasing wave amplitude, and, consequently, so do the local gas flow in the wave troughs and the intensification factor. For large $L > L_d$ the decay in Sh/Sh_0 occurs more slowly for large-amplitude waves. The effect of the wave length and of the fluid properties on mass exchange can be accounted for by means of the parameter εPe. The larger εPe is, the faster Sh/Sh_0 increases for $L \ll L_d$ and decreases for $L \gg L_d$.

What was said is also valid for chaotic regimes (see Fig. 6). Here, however, the presence of extended initial hydrodynamic and, consequently, mass-exchange portions leads to substantially lower Sh/Sh_0 values (for given L/λ) in comparison with the quasistationary two-dimensional wave regime.

In conclusion we note that within the concepts presented one can now understand and describe our data on mass exchange in a film as a function of its wave parameters, and explain inconsistent experimental results of other authors.

LITERATURE CITED

1. V. Beshkov and Khr. Boyadzhnev, "Effect of waves on mass transport during film flow," Izv. Khim. Bolg. Akad. Nauk, 11, 209 (1978).
2. V. E. Nakoryakov, B. G. Pokusaev, and S. V. Alekseenko, "Effect of waves on desorption of carbon dioxide gas from discharging fluid films," Teor. Osn. Khim. Tekhnol., 17, No. 3 (1983).
3. E. Ruckenstein and C. Berbente, "Mass transfer to falling liquid films at low Reynolds numbers," Int. J. Heat Mass Transfer, 11, No. 4 (1968).
4. P. I. Geshev and A. M. Lapin, "Diffusion of a weakly dissolved gas in discharging wave fluid films," Zh. Prikl. Mekh. Tekh. Fiz., No. 6 (1983).
5. V. E. Nakoryakov, B. G. Pokusaev, and I. R. Shreiber, Wave Propagation in Gas- and Vapor-Fluid Media [in Russian], ITF SO AN SSSR, Novosibirsk (1983).
6. K. B. Radev, "Conductive measurement method of studying mass exchange processes between phases in gas-fluid flows," in: Heat Mass Transfer in One- and Two-Phase Systems [in Russian], ITF SO AN SSSR, Novosibirsk (1983).
7. Z. Rotem and J. E. Neilson, "Exact solution for diffusion to flow down an incline," Can. J. Chem. Eng., 47, No. 3 (1969).
8. H. Sovová, "A correlation of diffusivities of gases in liquids," Coll. Czechoslov. Chem. Comm., 41, No. 12 (1976).
9. T. Ishihara, Y. Iwagak, and Y. Iwasa, "Discussion on roll waves and slug flows in inclined open channels," Trans. Amer. Soc. Civil Eng., No. 126 (1961).
10. S. Portalski, "Studies of falling liquid film flow. Film thickness on a smooth vertical plate," Chem. Eng., Sci., 18, No. 12 (1963).
11. I. A. Rogovaya, V. M. Olevskii, and N. G. Runova, "Measurement of parameters of film wave flow on a vertical plate," Teor. Osn. Khim. Tekhnol., 3, No. 2 (1969).
12. K. J. Chu and A. E. Dukler, "Statistical characteristics of thin wavy films," AIChE J., 21, No. 3 (1975).
13. V. E. Nakoryakov, B. G. Pokusaev, and S. V. Alekseenko, "Stationary two-dimensional rolling waves on a vertical fluid film," Inzh. Fiz. Zh., 30, No. 5 (1976).
14. N. N. Kulov and V. A. Malyusov, "Mass transfer in a tube with irrigation discharge and a mobile fluid film," Teor. Osn. Khim. Tekhnol., 1, No. 2 (1967).
15. P. I. Geshev, A. M. Lapin, and O. Yu. Tsvelodub, Heat and Mass Transfer in Wavy Discharging Films: Hydrodynamic and Mass Transfer in Flows with a Free Surface [in Russian], ITF SO AN SSSR, Novosibirsk (1986).